Regional and age-related variations of the healthy spinal cord structure assessed by multimodal MRI (diffusion, inhomogeneous magnetization transfer, ihMT)

Manuel Taso[1,2], Olivier M. Girard[3,4], Guillaume Duhamel[3,4], Arnaud Le Troter[3,4], Guilherme Ribeiro[3,4], Thorsten Feiweier[5], Maxime Guye[3,4], Jean-Philippe Ranjeva[3,4], and Virginie Callot[3,4]

[1]*CRMBM-CEMEREM UMR 7339, Aix-Marseille Université, CNRS, Marseille, France,* [2]*LBA UMR T 24, Aix-Marseille Université, IFSTTAR, Marseille, France,* [3]*CRMBM UMR 7339, Aix-Marseille Université, CNRS, Marseille, France,* [4]*CEMEREM, Pole d'imagerie médicale, Hopital la TImone, AP-HM, Marseille, France,* [5]*Siemens AG, Healthcare, Erlangen, Germany*

TARGET AUDIENCE Basic scientists and clinicians involved in spinal cord (SC) MR imaging, SC tissue characterization, and SC pathologies

INTRODUCTION Recent post-processing developments dedicated to SC MRI (SC template, registration procedure) (1,2) have opened new perspectives for robust group analyses and region-specific investigations. Meanwhile, new MR techniques have emerged and shown great promises for further SC tissue MR characterization, such as the recently proposed inhomogeneous magnetization transfer (ihMT) (3,4), which is a myelin specific technique. In this study, we propose to combine multimodal MRI (DTI and ihMT, to assess myelin and axonal content) and atlas-based analyses to study healthy SC structure spatial variations (interlevel/intralevel regions) and age effect on the SC structures. Thereby, a normative database useful for further SC pathologies investigations is also proposed.

MATERIAL AND METHODS ***MR scanning:*** 48 volunteers (26M/22F) were recruited and classified into 3 groups (age<35yo, n=17; 35<age<50, n=13 and age>50yo, n=18). MRI was performed at 3T (MAGNETOM Verio, Siemens Healthcare, Erlangen, Germany) using standard neck, head and spine matrix coils. **Anatomical imaging** consisted in an axial T_2*-w MEDIC (multi-echo GRE) sequence (ECG-gated, FOV 180x135mm^2, 0.5x0.5x5mm^3, 1 slice per cervical level, T_{acq}≈7min). **DTI** data were acquired with an ECG-gated monopolar single-shot SE-EPI prototype sequence (30 directions, 2 b-values (0-800 s/mm^2), fat suppression and local B_0 shimming, T_{acq}≈7min), at both C2 and C5 levels (FOV 128x128mm^2, 0.9x0.9x10mm^3). The DTI metrics (FA, ADC, $\lambda_{//}$ and $\lambda_{\perp}$) were calculated using Siemens Neuro 3D software. **Inhomogeneous Magnetization Transfer imaging** (3,4) was realized with a customized pulsed ihMT preparation (500 Hann-shaped pulses (500µs duration), repeated every 1ms, frequency offset f=7KHz, total saturation energy 12.1µT^2.s), using a single-slice HASTE readout (TR=4s, T_{acq}=8min), and by combining 4 different MT images according to ihMT=MT(+f)+MT(-f)–MT(+/-f)–MT(-/+f). Two axial acquisitions were performed at similar positions than DTI (FOV=172x172mm^2, resolution 0.9x0.9x10mm^3) and ECG data were recorded for retrospective filtering (5) before ihMT ratio (ihMTR) and conventional MTR maps reconstruction (ihMTR=ihMT/S_0, with S_0 the unsaturated free water image).

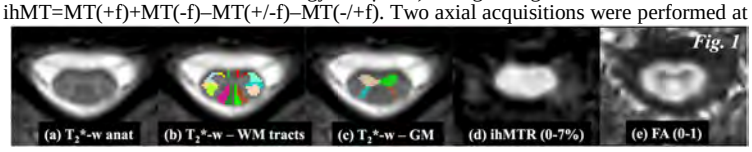

Post-processing: the SC was automatically segmented on the T_2*-w images using PropSeg (6), part of the Spinal Cord toolbox (http://sourceforge.net/projects/spinalcordtoolbox/) (2). Then, the SC mask (and the T_2*-w image) was registered to the AMU_{40} SC template (7) using 5DOF affine registration (FLIRT, FSL) (8). Once initialized, the T_2*-w image was non-linearly registered to the AMU_{40} T_2*-w template using ANTs (9) (SyN transform, cross-correlation cost function, 3rd order B-Spline interpolation). This was done independently for C2 and C5. Intra-subject registration was then performed between parametric MR (DTI/ihMT) and the corresponding T_2*-w slice using 4DOF affine registration. The multimodal metrics were finally normalized in the AMU_{40} space by using the warping field between the subject T_2*-w slice and the AMU_{40} template. Hence, metrics quantification was achieved in anterior GM and total WM (using the AMU_{40} thresholded (7) probabilistic WM/GM atlases), as well as in specific WM regions (lateral motor (LM) tracts, posterior sensory (PS) tracts and anterior motor (AM) tracts) derived from the recently proposed WM pathways atlas (part of the SC toolbox) (2,10). Statistical analyses (HSD Tukey-Kramer, JMP9, SAS) were conducted to highlight structural variations across regions and levels, but also to study the effect of age on multimodal metrics.

RESULTS AND DISCUSSION One example of T_2*-w (a), ihMTR (d) and FA (e) maps normalized to the AMU_{40} template is given on fig. 1 along with WM tracts (b) and GM ROI (c) derived from the different probabilistic atlases at C5.

Table 1

		ihMTR (%)			MTR (%)			FA			ADC (10^{-3} mm^2/s)			$\lambda_{//}$ (10^{-3} mm^2/s)			$\lambda_{\perp}$ (10^{-3} mm^2/s)		
Level	ROI	<50y.o	>50y.o	All ages	<50y.o	>50y.o	All ages	<50y.o	>50y.o	All ages	<50y.o	>50y.o	All ages	<50y.o	>50y.o	All ages	<50y.o	>50y.o	All ages
C2	Whole WM	5.79 ± 0.56	5.47 ± 0.56	5.67 ± 0.57	26.23 ± 3.08	25.77 ± 2.85	26.05 ± 2.96	0.72 ± 0.06	0.70 ± 0.04	0.71 ± 0.06	1.03 ± 0.09	0.99 ± 0.07	1.01 ± 0.08	2.04 ± 0.08	1.96 ± 0.10	2.01 ± 0.09	0.52 ± 0.13	0.50 ± 0.07	0.51 ± 0.11
	AM tracts	5.65 ± 0.78	5.44 ± 0.99	5.57 ± 0.87	27.56 ± 5.13	25.50 ± 6.77	26.75 ± 5.90	0.64 ± 0.08	0.65 ± 0.08	0.65 ± 0.08	1.03 ± 0.13	1.00 ± 0.15	1.02 ± 0.14	1.87 ± 0.15	1.84 ± 0.19	1.86 ± 0.17	0.61 ± 0.16	0.57 ± 0.15	0.60 ± 0.16
	LM tracts	6.03 ± 0.69	5.70 ± 0.71	5.90 ± 0.72	26.98 ± 3.28	26.22 ± 3.89	26.68 ± 3.54	0.69 ± 0.07	0.68 ± 0.05	0.69 ± 0.06	1.05 ± 0.11	0.99 ± 0.08	1.03 ± 0.11	2.01 ± 0.13	1.91 ± 0.12	1.97 ± 0.13	0.56 ± 0.15	0.53 ± 0.10	0.55 ± 0.13
	PS tracts	5.71 ± 0.63	5.26 ± 0.63	5.54 ± 0.67	25.91 ± 2.93	25.11 ± 3.47	25.59 ± 3.17	0.73 ± 0.07	0.71 ± 0.04	0.72 ± 0.06	1.07 ± 0.10	1.05 ± 0.08	1.07 ± 0.09	2.15 ± 0.13	2.07 ± 0.11	2.12 ± 0.13	0.54 ± 0.14	0.55 ± 0.09	0.54 ± 0.12
C5	Whole WM	5.08 ± 0.47	4.74 ± 0.42	4.98 ± 0.48	24.62 ± 1.47	23.07 ± 3.59	24.14 ± 2.38	0.67 ± 0.06	0.64 ± 0.05	0.66 ± 0.06	1.03 ± 0.10	1.06 ± 0.16	1.04 ± 0.12	1.94 ± 0.08	1.93 ± 0.12	1.94 ± 0.09	0.57 ± 0.13	0.63 ± 0.18	0.59 ± 0.15
	AM tracts	4.96 ± 0.68	4.84 ± 0.67	4.92 ± 0.68	24.83 ± 3.16	25.36 ± 2.35	25.00 ± 2.93	0.60 ± 0.07	0.59 ± 0.08	0.59 ± 0.07	1.02 ± 0.16	1.10 ± 0.22	1.05 ± 0.19	1.78 ± 0.26	1.86 ± 0.26	1.80 ± 0.26	0.64 ± 0.15	0.72 ± 0.23	0.67 ± 0.19
	LM tracts	5.42 ± 0.71	4.96 ± 0.53	5.28 ± 0.69	25.47 ± 2.74	23.67 ± 3.98	24.91 ± 3.27	0.64 ± 0.07	0.61 ± 0.06	0.63 ± 0.07	1.04 ± 0.11	1.07 ± 0.16	1.05 ± 0.13	1.89 ± 0.13	1.89 ± 0.15	1.89 ± 0.14	0.61 ± 0.13	0.67 ± 0.18	0.63 ± 0.15
	PS tracts	5.02 ± 0.66	4.64 ± 0.52	4.90 ± 0.64	24.02 ± 2.60	22.64 ± 4.17	23.60 ± 3.22	0.67 ± 0.07	0.64 ± 0.07	0.66 ± 0.07	1.09 ± 0.13	1.10 ± 0.16	1.09 ± 0.14	2.02 ± 0.13	1.96 ± 0.16	2.00 ± 0.14	0.62 ± 0.17	0.67 ± 0.19	0.64 ± 0.17

Multimodal metrics derived from DTI and ihMT acquisitions are summarized in table 1. When comparing C5 to C2 metrics (whole population), significant structural differences were found in the total WM, as clearly illustrated in fig.2c and d, with lower ihMTR ($p<0.0001$), FA ($p=0.0003$), MTR and $\lambda_{//}$ ($p=0.002$) and higher $\lambda_{\perp}$ ($p=0.02$) at C5. In the anterior GM, FA was found significantly lower at C5 (0.54±0.07 vs 0.46±0.07) $p<0.0001$).

When looking at WM tract-specific regions, the LM tracts presented higher ihMTR values than the PS and AM tracts ($p<0.0001$). Inversely, the PS tracts presented higher FA and $\lambda_{//}$ than both AM and LM tracts ($p<0.0001$) with however a similar $\lambda_{\perp}$.

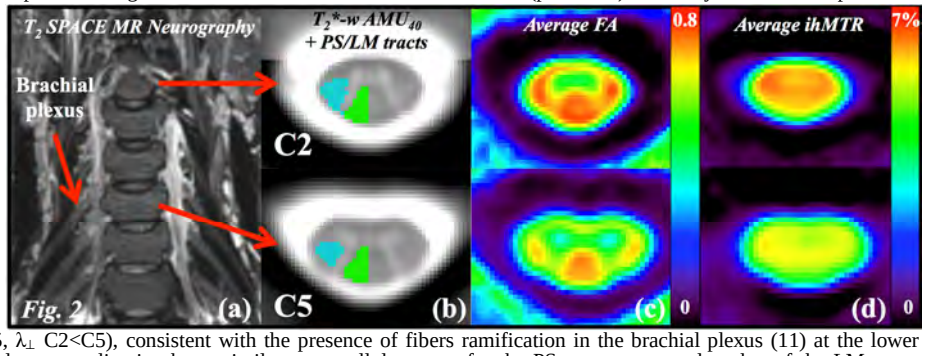

When studying the effect of age on the WM structure (in table 1, age groups<50 are combined for clarity), the ihMTR was found lower in the older age group at both levels and in both PS ($p=0.004$) and LM tracts ($p=0.006$). Similar observations were made for $\lambda_{//}$ ($p<0.05$), except in the LM and AM tracts at C5. $\lambda_{\perp}$ was also found significantly higher in the older age group in both AM and LM tracts at C5 ($p<0.04$). Finally, no difference could be observed in the GM, except a lower FA in aged group at C2 (0.55±0.07 vs 0.51±0.05, $p=0.05$).

Altogether, these results suggest: 1) higher myelin content and axonal density of the WM at the upper cervical levels (ihMTR C2>C5, FA C2>C5, $\lambda_{//}$ C2>C5, $\lambda_{\perp}$ C2<C5), consistent with the presence of fibers ramification in the brachial plexus (11) at the lower cervical levels (fig. 2a); 2) higher axonal density with lower myelination but a similar extra-cellular space for the PS tracts compared to that of the LM tracts (ihMTR PS<LM, FA PS>LM, $\lambda_{//}$ PS>LM, $\lambda_{\perp}$ PS≈LM) (fig. 2c, 2d), coherent with previous studies on animal models (12), as well as *ex vivo* (11) and *in vivo* (13) human studies ; and 3) an impairment of the SC WM structure with age, characterized by a substantial demyelination (higher $\lambda_{\perp}$ and lower ihMTR) and axonal loss (lower $\lambda_{//}$) for the older age group. Finally, these results also support the superior sensitivity of ihMT to depict demyelination compared to conventional MT, which did not show any significant variation, as well as the complementarity of DTI and ihMT to describe SC microstructure.

CONCLUSION In this study, regional differences of the SC structure were demonstrated, including differences between sensory and motor WM tracts and between upper and lower cervical SC levels. Modifications of the SC tissue (mainly axonal loss and demyelination) occurring with age have also been highlighted. Coherence with previously reported morphological alterations, such as GM atrophy (7,16), should be further investigated. Further work should also be directed towards the completion of the multimodal normative database along the whole spinal cord and across the entire lifespan, so as to be fully usable as reference when studying demyelinating and/or degenerative SC pathologies such as MS and ALS.

REFERENCES (1) Fonov et al, Neuroimage 2014; (2) Cohen-Adad et al, OHBM 2014; (3) Varma et al, MRM 2014; (4) Girard et al, MRM 2014; (5) Girard et al, ISMRM 2014; (6) De Leener et al, Neuroimage 2014; (7) Taso et al, ISMRM 2014; (8) Jenkinson et al, Neuroimage 2012; (9) Avants et al, Med. Image Anal. 2008; (10) Benhamou et al, ISMRM 2014; (11) Weil & Lassek, Archives of Neurology and Psychiatry, 1929; (12) Ong et al, Neuroimage 2008; (13) Duval et al, ISMRM 2014; (14) Agosta et al, Neuroimage 2007; (15) Vedentam et al, JMRI 2014; (16) Fradet et al, Spine 2014.